Princeton Plasma Physics Laboratory

PPPL- 4366

PPPL- 4366

Demonstration of Detuning and Wavebreaking Effects on Raman Amplification Effciency in Plasma

N. A. Yampolsky, N. J. Fisch, V. M. Malkin, E. J. Valeo, R. Lindberg, J. Wurtele, J. Ren, S. Li, A. Morozov, S. Suckewer

November, 2008

Prepared for the U.S. Department of Energy under Contract DE-AC02-76CH03073.

Princeton Plasma Physics Laboratory
Report Disclaimers

Full Legal Disclaimer

Trademark Disclaimer

PPPL Report Availability

Princeton Plasma Physics Laboratory:

http://www.pppl.gov/techreports.cfm

Office of Scientific and Technical Information (OSTI):

http://www.osti.gov/bridge

Related Links:

U.S. Department of Energy

Office of Scientific and Technical Information

Fusion Links

Demonstration of Detuning and Wavebreaking Effects on Raman Amplification Efficiency in Plasma

N. A. Yampolsky, N. J. Fisch, V. M. Malkin

Department of Astrophysical Sciences,

Princeton University, Princeton, New Jersey 08544, USA

E. J. Valeo

Princeton Plasma Physics Laboratory,

P.O. Box 451, Princeton, New Jersey 08543, USA

R. Lindberg, J. Wurtele

Department of Physics, University of California,

Berkeley, Berkeley, California 94720, USA

J. Ren, S. Li, A. Morozov, S. Suckewer

Department of Mechanical and Aerospace Engineering,

Princeton University, Princeton, New Jersey 08543, USA

A plasma-based resonant backward Raman amplifier/compressor for high power amplification of short laser pulses might, under ideal conditions, convert as much as 90% of the pump energy to the seed pulse. While the theoretical highest possible efficiency of this scheme has not yet been achieved, larger efficiencies than ever before obtained experimentally (6.4%) are now being reported, and these efficiencies are accompanied by strong pulse compression. Based on these recent extensive experiments, it is now possible to deduce that the experimentally realized efficiency of the amplifier is likely constrained by two factors, namely the pump chirp and the plasma wavebreaking, and that these experimental observations may likely involve favorable compensation between the chirp of the laser and the density variation of the mediating plasma. Several methods for further improvement of the amplifier efficiency in current experiments are suggested.

PACS numbers: 52.38.Bv, 42.65.Re, 42.65.Dr, 52.35.Mw

I. INTRODUCTION

Powerful short laser pulses have wide applications in physics, including wake field accelerators [1], fast ignition scheme of fusion [2], compact x-ray lasers [3], and compact terahertz sources [4]. Currently, short powerful laser pulses are generated using the chirped pulse amplification (CPA) technique. The CPA scheme is limited by fluency and intensity constraints on the solid state gratings. Currently, meter-scale gratings are used to produce PW-scale laser pulses.

Plasma-based laser amplifiers have been proposed as a means to circumvent the limits on the output power. One of the leading candidates for a next generation laser sources is the resonant backward Raman amplifier (BRA) [5]. In this scheme two counter-propagating laser pulses (which are called "pump" and "seed") interact with each other through the plasma wave, which is excited by the pondermotive force of beat wave. During the three-wave interaction the long pump transfers energy to the short seed pulse.

According to Manley-Rowe relations, the ratio of pump energy which can be transferred to the plasma wave is the ratio of the plasma to laser frequencies. This ratio is about a factor of 0.1 for typical parameters of BRA, $\omega_a/\omega_p \sim 1/10$. That means that almost all the energy of the pump (90% for $\omega_a/\omega_p = 1/10$) can be consumed by the seed pulse, while only 10% of the pump energy is absorbed to generate the plasma wave. [5–7]. Until recently, the experimentally achieved efficiencies were at most on the order of one percent [8–12]. However, recent experiments [13, 14] showed significantly enhanced amplification efficiency. This efficiency, on the order of several percent, remains much smaller than the theoretical maximum. Theoretical studies suggest a number of the mechanisms which may limit the efficiency of the scheme. The possible limiting mechanisms include resonance detuning from either a plasma density gradient or pump chirp [6], forward Raman and Brillouin scattering [15], amplified pulse self-focusing and self-phase-modulation [6, 16], small-scale density perturbations [17], the amplification of precursors [18], plasma wavebreaking [6, 19], thermal effects [20–22], and the ionization of low levels of the plasma ions [23]. The possible importance of the detuning and the wavebreaking in BRA experiments has been noted in earlier experiments [9]. However, the experimental data alone until now has not been sufficient to fully identify which effects, in fact, play the dominant role.

While the various factors mentioned above can all limit performance, the recent observa-

tions [14] are now comprehensive enough to constrain the possibilities. We show here that these observations exhibit an interplay between the pump chirp, the plasma density gradient, and the nonlinearity of the BRA interaction. We show that the pump chirp can be a leading limiting effect, and, moreover, that the pump chirp can be compensated by the plasma density gradient, as predicted by theoretical studies [6]. Furthermore, we demonstrate that the effect of detuning is power-dependent, becoming less important at high pump intensity. At the same time, we demonstrate that plasma wavebreaking at high pump intensity can be a dominant limiting factor in the BRA. Thus, we identify a pump intensity window for favorable amplification, and show that the recent experimental data apparently falls within this intensity window. These deductions follow from previously published results [13, 14] as well as new experiments which compare the "forward chirp" with the "reverse chirp".

The paper is organized as follows. In Sec. II we discuss experimental setup. In Sec. III we show that current data suggests that currently BRA operates in the linear regime accompanied with small pump depletion. In Sec. IV we discuss small efficiency of the amplifier caused by the pump chirp and the plasma density gradient. In Sec. V we discuss the wavebreaking of the plasma wave as one of the likely limiting effects in the experiment. In Sec. VI we identify the intensity window for BRA operation which is bounded by the influence of the detuning and the wavebreaking. Finally, in Sec. VII we present a number of techniques for increasing BRA efficiency in the experiment.

II. EXPERIMENTAL SET UP

The schematic of the experiment in [13, 14] is presented in Fig. 1. We focus here on just those features of the experiment which will be analyzed later in the paper; further details of the experiment and the full experimental results can be found in [13, 14]. Note that both the seed pulse and the pump pulse are generated by the same femtosecond Ti:Sapphire laser. The pulse is split into two pulses of different energies. Both the energies of the seed and the pump pulses can be varied by adjusting the Ti:Sapphire CPA laser system and can be controlled independently. The duration of the first pulse is controlled by CPA compressor C1 and is used as a pump pulse. The carrier frequency of the second pulse is downshifted using a Raman shifter. The pulse is then compressed in compressor C2, where it emerges as a seed pulse. The frequency difference between two pulses was optimized for resonant

three-wave interaction between the laser pulses and a plasma wave, which can be excited in pre-ionized recombining plasma.

The plasma is generated by ionization of a gas jet with 6 ns Nd:Yag laser pulse (called "prepulse"). A plasma channel technique is used [24] to generate a plasma column with good longitudinal homogeneity of the plasma density. The plasma density profile in the transverse direction is strongly nonuniform. The electron density at the boundary of the channel is about 1.4 times larger than at the center of the channel. The plasma density in the channel can be controlled by changing the time delay between the ionizing prepulse and the interacting pulses. This adjustment should enhance the amplification by matching the resonant condition of the three-wave interaction

$$\omega_a = \omega_b + \omega_p, \tag{1}$$

where ω_a and ω_b are the frequencies of the pump and the seed, respectively; $\omega_p = (4\pi e^2 n/m)^{1/2}$ is the plasma frequency.

The seed pulse has duration of about 500 fs and is focused inside the channel. It has almost uniform diameter of 55 μm along the channel. The spot size of the seed was controlled during its alignment without a plasma channel being created. The output spot size of the seed pulse cannot be measured in the presence of the plasma channel without the pump pulse, since no significant signal was observed. The spot size of the 20 ps pump was also controlled during the alignment without a plasma channel being created. The focal spot size of the pump is about $d^0_{pump} = 25$ μm. If the pump is focused at the exit from the channel, then the pump spot size at the entrance of the channel is about $d_{pump} = 50$ μm. This observation is consistent with diffraction of the Gaussian beam in vacuum

$$(d_{pump}/2)^2 = (d^0_{pump}/2)^2 \left(1 + \frac{4L^2c^2}{\omega_a^2 (d^0_{pump}/2)^4}\right), \tag{2}$$

where L is the length of the plasma channel. In the presence of plasma, the pump passes through the channel without being significantly damped (no seed pulse) losing about 10–15% of its energy. The spot size of the pump coming out from the plasma channel is almost the same as without plasma channel being created.

The transmission capacity of the pump (ratio of input and output energies) is much higher than the transmission capacity of the seed pulse. One question to answer is: why is the pump not damped, as opposed to the seed? The data suggests that the transmission capacity of

the laser pulses is a nonlinear process since the energy of the pump pulse is about 6000 times larger than the energy of the seed pulse and the power of the pump pulse is about a factor of 150 larger than the seed pulse power. It is possible that the linear side scattering of the pump due to plasma density perturbations is compensated by the nonlinear self-guiding. This self-guiding can be caused either by pondermotive or relativistic self-focusing of the pump beam. However, the pump power $P = 100$ mJ/20 ps=5×10^9 W is much smaller than the critical power for the relativistic focusing $P_{rel} = 1.7(\omega_a/\omega_p)^2 \times 10^{10}$ W $\approx 2 \times 10^{12}$ W [25]. At the same time, the pump power exceeds the critical power for its self-focusing due to the pondermotive force $P_{pond} = 1.15 \times 10^4$T[eV] W (for $T = 10$–1000 eV plasma) [26]. However, the duration of pump pulse is too short for the pondermotive self-focusing to develop on that time scale (a sound wave in 50 eV plasma travels a distance of 1.4 μm within the duration of the pump pulse which is much smaller than the pump spot size). Therefore, self-guiding of the pump is not likely to increase its transmission capacity. The most likely mechanism which could lead to larger pump transmission capacity but low seed transmission capacity is inverse bremsstrahlung absorption of the laser radiation. The partial absorption of the high energy pump might result in the increase of the plasma temperature which reduces inverse bremsstrahlung losses allowing the pump to be transmitted through the plasma channel. At the same time, the energy of the seed pulse is not high enough to increase the plasma temperature, so that strong damping of the seed is unaltered.

The recent experiments showed that enhanced seed amplification can be achieved using off-axis injection of the pump and the seed pulses with respect to the axis of the channel (Fig. 2). In this setup, both the amplified pulse power and the efficiency of amplification were increased by more than a factor of 4 compared to previous results [8]. This new data suggests that the improvement in efficiency is caused by the plasma density variation along the path of the pulses interaction.

The best amplification of the seed pulse was observed when the pump enters at about 5^o with respect to the channel axis. The path of the pump propagation is aligned so that the pump enters at 100 μm off the channel axis and exits at -100 μm off axis when it propagates in vacuum. However, the pump is refracted in the presence of the plasma channel, so it exits at -40 to -50 μm off the axis. The spot size of the pump at the exit from the plasma channel in the tilted experiments was slightly larger than in the axial experiments; it was measured as 25 μm $\times$ 40 μm. The seed pulse enters the channel slightly below the axis. The

amplified seed pulse exits the channel at 20–25 μm above the axis. Therefore, the seed pulse propagates at a much smaller angle than does the pump. Unfortunately, the shot-to-shot fluctuations in the seed profile preclude reliable estimates for the seed angle.

The exact paths of the pump and the seed propagation inside the channel are not measured experimentally. However, the entrance and exit positions of the pump are, so it appears that the pump propagates with an average 4^o angle within the channel. This angle is close to the incident 5^o angle of the pump in vacuum, which indicates that the pump refraction due to plasma density gradient is not large. The spot size of the pump at the exit from the channel is significantly smaller then the spot size $d_{pump} = 46$ μm which would be guided by a parabolic plasma density profile inside the channel [27]:

$$n(d_{pump}/2) - n(0) = \frac{4}{\pi d_{pump}^2 r_e}. \tag{3}$$

Here $r_e = e^2/(mc^2) = 2.8 \times 10^{-13}$ cm is classical electron radius. Therefore, the plasma density gradient does not refract the pump significantly and the pump propagation through the channel can be well approximated by vacuum diffraction. Refraction of the seed beam is smaller than refraction of the pump since it propagates closer to the channel axis. Although our knowledge of the pump and seed beams inside the channel is insufficient to compare in detail to theoretical studies of the resonant BRA in plasma channels [28–30], the main conclusions of our paper are independent of these details.

III. COMPARISON OF EXPERIMENTAL DATA WITH BRA THEORY

Neglecting then focusing and refraction effects, the backward Raman Amplification effect can be described adequately n terms of a set of equations for the wave envelopes [5, 6]:

$$a_t + ca_z = -\sqrt{\omega\omega_p} bf \tag{4}$$

$$b_t - cb_z = \sqrt{\omega\omega_p} af^* \tag{5}$$

$$f_t - i\delta\omega f = \sqrt{\omega\omega_p} ab^*/2, \tag{6}$$

where a, b are the amplitudes of the pump and the seed, respectively, normalized so that the laser intensity $I_a = \pi c(mc^2/e)^2|a|^2/\lambda^2 = 2.736 \times 10^{18}|a|^2/\lambda^2[\mu m]$ W/cm^2; f is appropriately normalized amplitude of the plasma wave; $\delta\omega$ is the detuning frequency between the waves

which is caused by failure of exact resonant condition (1); t is time and z is longitudinal coordinate along the direction of the pump propagation.

The advanced stage of amplification is accompanied by pulse compression, which assumes a self-similar form. We call this regime "advanced" in order to distinguish it from the initial linear stage of amplification, which is accompanied by the exponential growth of the amplified pulse amplitude and an increase in its duration rather than a decrease. In the advanced regime, the evolution of the waves can be described well by a set of equations reduced from (4) — (6) [6].

$$a_\zeta = -bf \tag{7}$$

$$b_\tau = af^* \tag{8}$$

$$f_\zeta - ia_0^2 q\tau f = ab^*, \tag{9}$$

where $\zeta = (t + z/c)\sqrt{\omega_a\omega_p}/2$ is the normalized longitudinal coordinate behind the seed pulse and $\tau = -z\sqrt{\omega_a\omega_p}/c$ is the normalized amplification length, $q = 2(\partial_z\omega_p - 2\partial_z\omega_a)c/(a_0^2\omega_a\omega_p)$ is the detuning factor.

This set of equations allows a self-similar solution [6] having the following form

$$b = a_0^2\tau B(a_0^2\zeta\tau) \tag{10}$$

$$a = a_0 A(a_0^2\zeta\tau), \qquad f = a_0 F(a_0^2\zeta\tau)\ . \tag{11}$$

In this regime the maximum amplitude of the amplified pulse, $b_{\max}(\tau)$, grows linearly with the amplification length while its duration decreases inversely proportional with the amplification length; $b_{max} \propto \tau$, $\Delta\zeta \propto 1/\tau$. This scaling remains even if strong detuning is present [6, 31] and was observed in current experiments [8, 13].

The compression of the amplified pulse at the advanced stage of amplification produces a corresponding increase in its spectral width. The amplified pulse can be spectrally broadened either through nonlinear compression effect [5], or through chirps in the pump, or density gradient in the plasma [31]. In this case, a simple analysis using Fourier transform of the equations is no longer applicable, since various harmonics of the pulse become coupled. Both the nonlinearity and the detuning from the resonance condition are present in the BRA equations (7) — (9). Therefore, both effects can contribute to the experimental observations in Fig. 4. BRA was proposed [5] to operate in the nonlinear regime, where pulse compression is caused by nonlinearity due to pump depletion. However, detuning can significantly reduce

pump depletion, in which case the evolution of the amplified pulse can be described in terms of linear equations. But this detuning itself results in spectrally broadened output pulse.

It was previously suggested that the nonlinear stage of amplification, accompanied by noticeable pump depletion, was reached [8]. An increase of the amplified pulse bandwidth, suggesting pulse compression, and linear growth of the pulse energy with the pump energy was noted. However, the observations of increased bandwidth can also be explained by detuning. New autocorrelation measurements (Fig. 3) and new scaling (Fig. 4) also support both scenarios, namely, either the achievement of the nonlinear stage or the influence of detuning [13, 14]. The scaling in Fig. 4 was fitted using least square fit with a function $W^{\alpha}\Delta t = const$, where W and Δt are the amplified pulse energy and duration, respectively. The experimentally deduced $\alpha = 0.7$ does not quite agree with BRA theory for fully asymptotic amplified pulses, for which $\alpha = 1$, but neither does the experimental accuracy rule out consistency with the theoretical limit.

The self-similar solution, Eqs. (10) — (11), appears at the advanced stage of amplification. It has a spiked structure [5, 6]. The first spike of the amplified pulse has about 50% of the total pulse energy for typical seed parameters. The integral over the first spike of the amplified pulse amplitude should be somewhat smaller than π in the advanced regime of amplification [6]. The detuning and the plasma wavebreaking mostly result in the suppression of the secondary spikes. The leading spike is also modified by these mechanisms but its integrated amplitude should remain at the same order of magnitude. A simple estimate for the output seed pulse parameters in the axial experiments is (pulse duration $\Delta t = 90$ fs, energy in the first spike $W = 1.45$ mJ, pulse spot size is 15 μm $\times$ 20 μm):

$$\int b d\zeta \approx 0.6\pi. \tag{12}$$

This value is close to theoretical predictions. This fact, combined with the scaling in Fig. 4, suggests that the advanced stage of amplification actually has been reached. However, it does not definitely indicate that the nonlinear stage of amplification has been reached.

This uncertainty might be resolved by measuring indirectly the pump depletion rate. Although, the amplified pulse extracts pump energy in the domain of their temporal and spatial overlap, the average pump depletion rate can be estimated indirectly, taking into account that only some fraction of the pump is used for the seed amplification. We neglect the seed diffraction and estimate its spot size to be 15 μm along the channel (the spot size of

the output seed). Consistent with the roughness of this calculation, we neglect the increase in the amplified pulse intensity that might be due to linear or nonlinear focusing of the seed beam while it travels along the channel. We also assume that there are no additional losses associated with the imperfect alignment of the pump and seed. Taking into account the pump intensity profile along the channel due to vacuum diffraction (assuming that the pump is focused at 3/4 of the channel length), we arrive at an estimate of the average fractional depletion of the pump

$$D_{pump} = \frac{W_{seed}}{\pi d_{seed}^2/4 \int\limits_0^{L_{plasma}} 2I_{pump} dz/c}. \tag{13}$$

The experimental data presented in upper plot of Fig. 6 suggests that the average fractional depletion of the pump $D_{pump} = 0.12$ for axial experiments and $D_{pump} = 0.4$ for tilted experiments. This estimate suggests that the pump is not fully depleted in the experiment. In axial experiments, the depletion of the pump is much smaller than unity, which suggests that the nonlinear stage of amplification has not been reached. Although, the tilted experiments show significantly larger pump depletion, the pump is still not fully depleted, which suggests the presence of mechanisms which saturate BRA.

In the following sections, we show that the data points to two primary mechanisms, namely detuning and the plasma wavebreaking, which are likely to cause the reduced pump depletion. The detuning introduces a phase shift between the waves. That dephasing reduces amplification and can even result in the energy transfer from the amplified pulse back to the pump. The plasma wavebreaking limits the amplitude of the plasma wave which can be supported by plasma. As a result, the coupling between the laser waves in Eqs. (4) — (6) vanishes.

IV. DETUNING

The detuning can be characterized by the dimensionless parameter

$$q = \frac{2(\partial_z \omega_p - 2\partial_z \omega_a)c}{a_0^2 \omega_a \omega_p}, \tag{14}$$

where a_0 is the undepleted amplitude of the pump. It describes the growth rate of the detuning frequency in the frame moving with the amplified pulse $\delta\omega \propto q(t+z)$ in (4) — (6).

There are two primary mechanisms which can drive the interaction away from the optimum resonance condition, namely exact resonance. The detuning can be caused either by the plasma density gradient or by the pump chirp. These two detunings can compensate each other so that in the frame moving with the front of the seed pulse the resonant frequency of the seed remains constant.

The detuning caused by the pump chirp can significantly reduce pump depletion in the axial experiments when the seed pulse is amplified in uniform plasma. The pump pulse is chirped since it comes from the CPA amplifier. It is compressed by gratings from 240 ps to 20 ps, which does not fully remove the chirp (if it was compressed to the minimum pulse duration of 100 fs, the chirp would be absent). The pump chirp can be approximated as linear at 12 nm/800 nm=1.5% over 20 ps. The dimensionless parameter which describes detuning is then:

$$q_{pump} = \frac{4\omega' c}{\omega_p \omega a_0^2} \approx 0.27 \tag{15}$$

for the pump intensity $I_{\text{pump}} = 2.3 \times 10^{14}$ W/cm^2, which is the estimated pump intensity at the entrance to the plasma channel. Since the detuning parameter is inversely proportional to the pump intensity, $q \sim I_{\text{pump}}^{-1}$, the detuning q is relatively small at the focal spot of the pump, since the pump intensity there is about 6 times larger than at the edge of the channel. Here we assume that the focusability of the pump is not significantly affected by the presence of the plasma channel. At the same time, the pump chirp might limit the pump depletion at the edge of the plasma where the pump intensity is not large enough. Note that this effect should be taken into account when planning future experiments which rely on chirp compensation.

Detuning results in incomplete pump depletion, which, in turn, limits the efficiency of the BRA. Predicting the exact pump depletion rate is difficult because the rate depends on the integrated amplitude of the short original seed pulse through $\epsilon = \sqrt{\omega_a \omega_p} \int b_0 dt$ (Fig. 7 of [6]). However, if the original seed pulse is longer or the order on the amplified pulse, then only a small fraction of the seed pulse plays a role in BRA. The back part of the seed is shadowed by its front and does not affect amplification [32, 33]. In this case, the effective seed pulse amplitude ϵ_{eff} is a useful concept [32]. The original seed pulse has a large enough integrated amplitude $\epsilon \approx 0.1$, but the effective seed amplitude can be reduced by several orders of magnitude during amplification. Such an effective reduction of the seed amplitude

can result in significant reduction of the BRA efficiency.

The effective seed amplitude, ϵ_{eff}, strongly depends on the profile of the seed front. The seed pulse is formed by the CPA compressor after being modified in the Raman shifter. Seeds generated in such a way can have small variations, but result in very different output pulses. To see this, we compare, in Fig. 5, the output pulse for a Gaussian seed pulse (upper plot) with the output pulse for a Gaussian seed pulse with tails truncated when they reach 20% of the maximum amplitude (lower plot). Fig. 5 shows simulated output pulses corresponding to the axial experiments in which the detuning is not compensated. The output pulse duration should not be compared with autocorrelation measurement at Fig. 3, since those are done for tilted experiments. While the simulations shown in Fig. 5 do not fully reproduce in detail the experimental data (since the longitudinal dependence of the detuning and the pump intensity as well as seed diffraction were not taken into account) these simulations nevertheless exhibit the tendency for better amplification using a seed pulse with a sharp front.

The detuning caused by the pump chirp can be partially compensated by detuning caused by the plasma density gradient. Such a density gradient can be introduced if two laser pulses propagate at an angle with respect to the channel axis. In this setup, the plasma frequency changes along the interaction path, since the channel has a transverse density gradient. In fact, such a setup showed an increased output pulse energy from 2 mJ to 6.4 mJ (upper plot of Fig. 6). The maximum output pulse energy was observed for a 4^o average tilt angle inside the channel. The detuning parameter, q_{plasma}, caused by the plasma density gradient, for this angle of 4^o is

$$q_{plasma} = \frac{2\omega_p' c}{\omega_p \omega a_0^2} \approx 2.3. \tag{16}$$

Here we took the plasma density to change from $2 \cdot 10^{19}$ cm^{-3} to $1.4 \cdot 10^{19}$ cm^{-3} within ~ 500 μm propagation distance.

This detuning is much larger than the detuning caused by the pump chirp. However, the detuning factor q_{plasma} should correspond to the plasma density change along the path of the seed beam rather than the path of the pump beam. The tilt angle of the seed beam is much smaller than the tilt angle of the pump beam (as described in Sec. II) which results in a significantly reduced value of q_{plasma}. Unfortunately, the exact value of the seed tilt angle cannot be deduced from the experimental data. Moreover, interferometer measurements of

the plasma density (Fig. 2) are not accurate close to the axis of the plasma channel. These factors do not allow one to make reliable estimates of the detuning q_{plasma} along the path of the seed beam. It is also not quite clear why the maximum seed amplification would be observed if the tilt angle of the pump beam were much larger than the tilt angle of the seed beam.

Although lacking an accurate estimate of q_{plasma} in the overlap region, we can deduce the detuning compensation by changing the sign of the pump chirp. It is critical to note that the enhanced pump depletion in experiments with tilted alignment of the laser beams can be observed only if the detunings have opposite signs and cancel each other. In these experiments the pump chirp was positive (the pump frequency increases in time). Therefore, the detuning compensation is possible only on the left side of the plasma channel (Fig. 2). While the amplified pulse travels in that region, the pump frequency increases in time, as does the encountered plasma density (the pump enters the channel from the left and the seed enters the channel from the right). Therefore, the two detunings compensate each other. On the other hand, the plasma density gradient destructively interferes with the pump chirp on the right-hand side of the channel. However, the pump is set up to be focused near the exit plane of the channel in vacuum. This focus should be retained in the presence of plasma, since the pump is not significantly refracted or focused by the channel. Therefore, the detuning factor q is relatively smaller on the right side of the channel, since the pump intensity is larger in that domain. Moreover, the position of the seed beam in respect to the channel axis can be different in two domains of the plasma channel. That can result in smaller density gradient and reduced effect of detuning in the right-hand side of the channel. Therefore, the experimental arrangement with tilted alignment of the laser beams is more favorable than the arrangement with no tilt, or exactly axial propagation.

The detuning importance can be demonstrated experimentally by reversing the pump chirp, as seen in Fig. 6. (The upper and lower plots in Fig. 6 correspond to slightly different experimental setups and the experiments were done at different times. Therefore, any precise comparison of these data should be done with caution.) In the experiments with negative (reversed) pump chirp (lower plot), the efficiency in tilted experiments is smaller than the efficiency in axial experiments. This tendency is opposite to the experiments with positive pump chirp (upper plot). That means that the sign of the pump chirp is very important for BRA efficiency. Reduced efficiency of the amplification can be explained as

destructive interference of the detunings due to the pump chirp and the plasma density gradient. Flipping the sign of the pump chirp results in addition of the detunings rather than their compensation. The overall detuning factor q increases and the efficiency drops down significantly.

V. PLASMA WAVEBREAKING

Another mechanism which can prevent full pump depletion is plasma wavebreaking. The critical pump intensity I_{cr} which leads to the plasma wavebreaking in BRA can be estimated [6] as

$$\frac{\omega_p}{\omega_a} = (4a_0)^{2/3} \quad \Leftrightarrow \quad I_{cr} = 1.8 \cdot 10^{14} \mathrm{W/cm}^2. \tag{17}$$

This is the estimate for cold plasma; finite plasma temperature can significantly reduce this threshold. Although, there is no precise analytical model for the wavebreaking, an estimate based on the "water-bag" model [34] shows that the critical intensity is reduced by a factor of 6 for 20 eV plasma. A higher plasma temperature results in an even smaller critical intensity for the plasma wavebreaking. Several empirical models of the plasma wavebreaking in cold plasma in BRA were introduced in [9]. Other warm plasma descriptions of Raman saturation via the nonlinear modification of the electron distribution function and particle trapping have been proposed by, e.g., [35–37]. Comprehensive modeling of including wavebreaking is difficult since many plasma wavelengths should be taken into account (17 plasma wavelengths within 500 fs pulse, 5000 wavelengths within channel length) and requires extensive numerical simulations [38]. For our purposes the cold plasma limit suffices to identify an upper intensity limit to what will become a window of operation in intensity space.

The intensity of the pump is close to its critical value at the boundary of the plasma (at the side where the pump enters plasma). At the focal spot, the pump intensity exceeds the critical value by a factor of 6. Thus, wavebreaking prevents full pump depletion, since the amplitude of the plasma wave cannot exceed its critical value. Numerical calculations of wavebreaking in cold plasma suggest that only about 50% of the pump can be depleted in the focal spot domain. In warm plasma, only a smaller fraction of the pump can be depleted. Therefore, plasma wavebreaking can be a reason for inefficient energy transfer from the pump to the seed pulse.

Note that the largest amplification is observed when the pump is focused closer to the boundary at which the seed enters the plasma. In this case the seed sees a pump intensity decreasing in time. First, it is amplified in the domain in which the wavebreaking can potentially happen. However, in this domain, the amplitude of the seed is small and it can be amplified linearly without reaching the wavebreaking limit. When the seed amplification reaches the nonlinear stage, it encounters a near-critical pump intensity where wavebreaking does not prevent an almost complete pump depletion. If the focal spot were located closer to pump entrance into plasma, the wave breaking would limit the amplification, since the nonlinear regime would then be driven by the overcritical pump.

The enhanced amplification of the seed in the experiments with tilted geometry of the beams could be caused by reduced influence of the plasma wavebreaking. In these experiments, the spot size of the output seed is larger than if the beams were aligned axially. The diameter of the seed pulse in "'y" direction is about a factor of 1.6 larger than in "'x" direction. This fact can be caused by increased focal spot of the pump due to refraction (different angular harmonics of the pump refract slightly different which can affect the change of the focal spot size). In the wavebreaking regime the same pump fluency can be consumed by the seed. That results in increased total energy which can be extracted from the pump.

The position of the focal spot of the pump was varied over a broad range in the experiment. The pump was even focused outside the plasma which resulted in large spot size of the pump within the channel. Thus, the intensity of the pump was reduced within the interaction region. In these experiments, the wavebreaking limit might not be reached, so the amplified seed energy should have increased. Yet increased efficiency is not observed in the experiments in which the pump is focused outside the plasma channel. The decrease in efficiency is due to the detuning which is larger at low pump intensity, as we proceed to consider in the next section.

VI. PUMP INTENSITY WINDOW FOR BRA

The pump intensity window for efficient backscatter is bounded by two primary mechanisms, namely detuning and plasma wavebreaking. These mechanisms dominate in different regions of the plasma channel. The plasma wavebreaking limits the amplification at high pump intensity while the detuning becomes important at low pump intensity. Therefore,

there is a parameter region for the pump intensity which is favorable for BRA. This idea is illustrated in Fig. 7. Here we plot individual efficiencies due to the detuning and the plasma wavebreaking. The BRA efficiency due to the wavebreaking is taken from the assumption that only critical pump intensity (17) can be absorbed. Further absorption of the pump leads to the plasma wavebreaking and cancels the interaction. The pump depletion rate caused by the detuning was calculated in [6]. The overall efficiency of BRA is assumed to be a product of partial efficiencies due to the detuning and the plasma wave breaking. Although a detailed comparison of the experimental and the theoretical efficiency plots is complicated since the pump has nonuniform intensity profile along the channel, the effects of detuning and wavebreaking are robust and the dependence of the BRA efficiency versus pump energy can still be observed. The experimentally observed efficiency has the same kind of intensity dependence as predicted theoretically. This dependence was observed experimentally for the first time. The precise boundaries of this window are not to be understood qualitatively since they would depend on the precise overlap between the pump and the seed and the plasma temperature, neither of which we know very precisely experimentally in any event.

Thus, the experimental data supports the theoretical assumption that both the detuning and the plasma wavebreaking limit the BRA efficiency in the experiment. Moreover, the overall efficiency is the largest in the regime in which these two limiting effects are competing with neither dominant. However, in the current set up this efficiency is significantly smaller than unity. Since the efficiency limit due to the plasma wavebreaking cannot be changed for a given plasma density and pump intensity, what then remains available to increase the overall BRA efficiency is to reduce the detuning. This possibility was demonstrated experimentally using tilted geometry of the interacting laser pulses. However, in the current set up, since the sign of the pump chirp is constant and the sign of the plasma density gradient changes when the interaction path crosses the axis of the channel, the pump chirp can be compensated only in a limited region of the plasma channel. Therefore, the detuning cannot be fully compensated in the setup considered in [13]. To fully compensate the pump chirp, a plasma with constant density gradient would be required. The undesirable detuning caused by the plasma density gradient in the right-hand side of the channel can also be reduced if the seed beam is significantly refracted by the channel which causes its almost axial propagation in that domain.

VII. IMPROVED EFFICIENCY BY SUPPRESSING DETUNING

Having identified a window of high efficiency, we now offer suggestions for improved efficiencies. Since detuning plays an important role at small pump intensity, while wavebreaking dominates at high pump intensity, these two effects cannot be avoided simultaneously by going to higher or lower pump power. The efficiency of BRA can be enhanced only by reducing the gradients of the interacting wave frequencies.

The effect of detuning can be reduced in a number of ways. In principle, the pump chirp can be eliminated, in which case the plasma should be uniform. But the pump pulse comes out from the CPA amplifier and necessarily has a frequency chirp. This chirp can be reduced by additional stretching out the pump pulse. Then, if the pump frequency gradient is small, then so is the detuning factor q. However, this technique requires the use of a longer pump pulse which eventually reduces the overall efficiency, since only a small portion of the pump is utilized for the seed amplification. A longer plasma channel is then required in order to provide interaction with the full pump.

The chirp of the pump can also be reduced by using a pump of a smaller bandwidth. In this case the stretched out pump pulse has a smaller frequency difference from the front to the back. In this case the CPA laser should be modified so that the seeding pulse for the pump (the seeding pulse which is amplified in the CPA amplifier, not the one which is amplified later in plasma) has smaller bandwidth. However, this technique does not allow one to use a single laser system to produce both the pump and the seed pulses for BRA since the seed pulse should have large bandwidth in order to be short.

The effect of detuning can also be reduced if the seed pulse of larger integrated amplitude ϵ_{eff} is used. Earlier research [6] showed that the pump depletion rate depends logarithmically on the integrated seed amplitude ϵ_{eff}. Therefore, increasing the seed amplitude will not result in a large enhancement of BRA efficiency. At the same time, effective seed pulse amplitude ϵ_{eff} strongly depends on the seed duration since only small domain at the seed front influences BRA. For a Gaussian seed, the effective integrated seed amplitude depends exponentially on the seed duration [32]. Therefore, the use of shorter seed pulses will significantly reduce the effect of detuning.

The effective integrated seed amplitude ϵ_{eff} can also be reduced by increasing the slope of the seed front. This can be done by passing the seed through an absorbent with sat-

uration. Such a technique allows one to eliminate low amplitude front of the seed pulse which determines ϵ_{eff} at the advanced stage of amplification. As a result, ϵ_{eff} of this seed pulse reduces much slower than ϵ_{eff} of the Gaussian seed pulse. Therefore, the effect of the detuning can be suppressed which leads to the enhanced BRA efficiency (see Fig. 5).

Finally, the detuning can be reduced if the pump chirp is compensated by the plasma density gradient. The attraction is that the CPA laser need not be modified and the full pump is used for BRA. However, creating a plasma with a constant density gradient is technologically challenging. We suggest, however, that the plasma can be created in a gas jet that spreads out from the nozzle. The gas density is large close to the nozzle and becomes small far from the nozzle. Originally the plasma channel was created parallel to the nozzle so that the plasma density was uniform. If the channel is created at some angle to the nozzle, then the gas density, or plasma density, in fact varies along the channel.

VIII. SUMMARY

We identified the key mechanisms for limiting the efficiency in recent Raman compression experiments. We also identified an intensity window for favorable operation. The detuning caused by the pump chirp and the plasma density gradient are the main limiting effects at low pump intensity. On the other hand, seed amplification at high pump intensity is ineffective due to the plasma wavebreaking.

We showed that the large pump chirp generated by a broadband CPA laser, with dimensionless detuning parameter $q_{pump} \approx 0.27$, is large enough to detune the 3-wave resonance. As a result, amplification in uniform plasma is accompanied by a low pump depletion rate. Experiments with tilted alignment of the laser beams result in enhanced BRA efficiency, which occurs through the partial compensation of the pump chirp by an effective chirp due to the plasma density gradient. To support this explanation, experiments with reversed sign of the pump chirp were performed which in fact showed reduced seed amplification.

The effect of the detuning becomes less significant at high pump intensity. At the same time, the effect of the plasma wavebreaking becomes more significant at high pump intensity. Therefore, the BRA efficiency reaches its maximum at a certain pump intensity for a given pump chirp and plasma density gradient. At higher pump intensities, plasma wavebreaking tends to dominate, suggesting a window of operation for efficient backward Raman ampli-

fier. We showed that the experimental results support the identification of the window of operation.

IX. ACKNOWLEDGEMENTS

This work supported by the NNSA under the SSAA Program through DOE Research Grant No. DE-FG5207NA28122 and by DOE Contract DE-AC02-76CH03073.

---

[1] T. Katsouleas, Phys. Plasmas **13**, 055503 (2006).

[2] M. Tabak, D. Hinkel, S. Atzeni, E. M. Campbell, and K. Tanaka, Fusion Sci. and Tech. **49**, 254 (2006).

[3] Y. Avitzour and S. Suckewer, J. Opt. Soc. Am. B **24**, 819 (2007).

[4] T. Loffler, M. Kress, M. Thomson, T. Hahn, N. Hasegawa, and H. G. Roskos, Semicond. Sci. and Tech. **20**, S134 (2005).

[5] V. M. Malkin, G. Shvets, and N. J. Fisch, Phys. Rev. Lett. **82**, 4448 (1999).

[6] V. M. Malkin, G. Shvets, and N. J. Fisch, Phys. Plasmas **7**, 2232 (2000).

[7] N. J. Fisch and V. M. Malkin, Phys. Plasmas **10**, 2056 (2003).

[8] W. Cheng, Y. Avitzour, Y. Ping, S. Suckewer, N. J. Fisch, M. S. Hur, and J. S. Wurtele, Phys. Rev. Lett. **94**, 045003 (2005).

[9] A. A. Balakin, D. V. Kartashov, A. M. Kiselev, S. A. Skobelev, A. N. Stepanov, and G. M. Fraiman, JETP Lett. **80**, 12 (2004).

[10] R. K. Kirkwood, E. Dewald, C. Niemann, N. Meezan, S. C. Wilks, D. W. Price, O. L. Landen, J. Wurtele, A. E. Charman, R. Lindberg, N. J. Fisch, V. M. Malkin, and E. O. Valeo, Phys. Plasmas **14**, 113109 (2007).

[11] C.-H. Pai, M.-W. Lin, L.-C. Ha, S.-T. Huang, Y.-C. Tsou, H.-H. Chu, J.-Y. Lin, J. Wang, and S.-Y. Chen, Phys. Rev. Lett. **101**, 065005 (2008).

[12] M. Dreher, E. Takahashi, J. Meyer-ter-Vehn, and K.-J. Witte, Phys. Rev. Lett. **93**, 095001 (2004).

[13] J. Ren, W. Cheng, S. Li, and S. Suckewer, Nature Phys. **3**, 732 (2007).

[14] J. Ren, S. Li, A. Morozov, S. Suckewer, N. A. Yampolsky, V. M. Malkin, and N. J. Fisch, Phys. Plasmas **15**, 056702 (2008).

[15] V. M. Malkin, Y. A. Tsidulko, and N. J. Fisch, Phys. Rev. Lett. **85**, 4068 (2000).

[16] G. M. Fraiman, N. A. Yampolsky, V. M. Malkin, and N. J. Fisch, Phys. Plasmas **9**, 3617 (2002).

[17] A. A. Solodov, V. M. Malkin and N. J. Fisch, Phys. Plasmas **10**, 2540 (2003).

[18] Y. A. Tsidulko, V. M. Malkin, and N. J. Fisch, Phys. Rev. Lett. **88**, 235004 (2002).

[19] G. Shvets, N. J. Fisch, A. Pukhov, and J. Meyer-ter-Vehn, Phys. Rev. Lett. **81**, 4879 (1998).

[20] R. L. Berger, D. S. Clark, A. A. Solodov, E. J. Valeo, and N. J. Fisch, Phys. Plasmas **11**, 1931 (2004).

[21] H. X. Vu, L. Yin, D. F. DuBois, B. Bezzerides and E. S. Dodd, Phys. Rev. Lett. **95**, 245003 (2005).

[22] M. S. Hur, R. R. Lindberg, A. E. Charman, J. S. Wurtele, and H. Suk, Phys. Rev. Lett. **95**, 115003 (2005).

[23] A. A. Balakin, G. M. Fraiman, N. J. Fisch, and S. Suckewer, Phys. Rev. E **72**, 036401 (2005).

[24] C. G. Durfee III, J. Lynch, and H. M. Milchberg, Phys. Rev. E **51**, 2368 (1995).

[25] A. G. Litvak, Zh. Eksp. Teor. Fiz. **57**, 629 (1969) [Sov. Phys. JETP **30**, 344 (1970)]; C. Max, J. Arons, and A. B. Langdon, Phys Rev. Lett. **33**, 209 (1974); Guo-Zheng Sun, E. Ott, Y. C. Lee, and P. Guzdar, Phys. Fluids **30**, 526 (1987).

[26] H. Hora, Z. Physik **226**, 156 (1969).

[27] P. Sprangle and E. Esarey, Phys. Fluids B **4**, 2241 (1992).

[28] P. Mardahl, H. J. Lee, G. Penn, J. S. Wurtele, and N. J. Fisch, Phys. Lett. A **296** , 109 (2002).

[29] I. Y. Dodin, G. M. Fraiman, V. M. Malkin, and N. J. Fisch, J. Expt. Theor. Phys **95**, 625 (2002).

[30] S. Yu. Kalmykov and G. Shvets, Phys. Plasmas **11**, 4686 (2004).

[31] B. Ersfeld and D. A. Jaroszynski, Phys. Rev. Lett. **93**, 095001 (2004).

[32] N. A. Yampolsky, V. M. Malkin, and N. J. Fisch, Phys. Rev. E **69**, 036401 (2004).

[33] M. S. Hur, D. N. Gupta, and H. Suk, J. Phys. D - Appl. Phys. **40**, 5155 (2007).

[34] T. P. Coffey, Phys. Fluids **14**, 1402 (1971).

[35] H. X. Vu, D. F. DuBois, and B. Bezzerides, Phys. Plasmas **14**, 012702 (2007).

[36] D. Benisti, D. J. Strozzi, and L. Gremillet, Phys. Plasmas **15**, 030701 (2008).

[37] R. R. Lindberg, A. E. Charman, and J. S. Wurtele, Phys. Plasmas **15**, 055911 (2008).

[38] D. S. Clark and N. J. Fisch, Phys. Plasmas **10**, 4848 (2003).

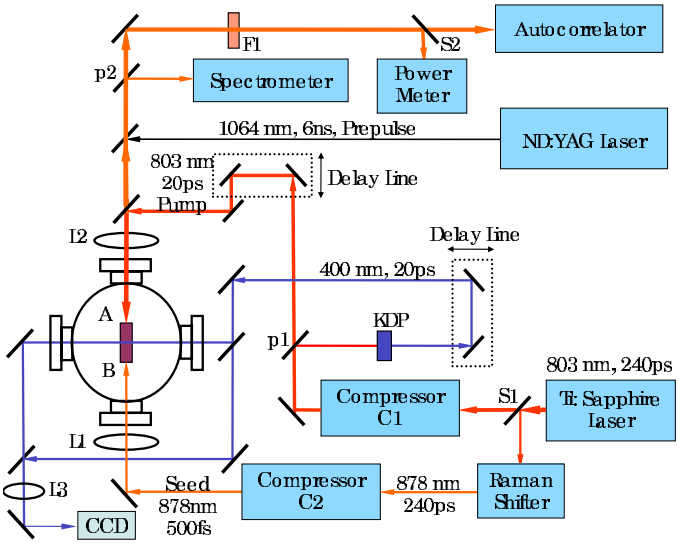

FIG. 1: (Color online) The experimental scheme of the backward Raman amplifier described in [13,14]. The seed pulse after splitter S1 goes through Raman shifter, compressor C2 and enters the vacuum chamber from below. The pump pulse after splitter S1 goes through compressor C1 and enters the chamber from above.

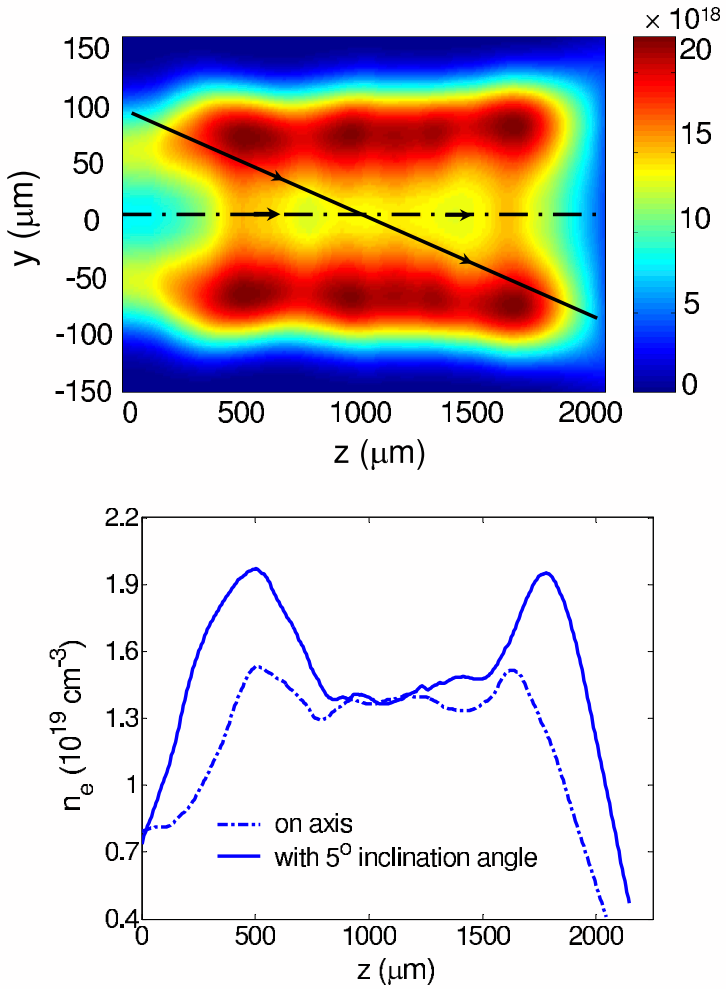

FIG. 2: (Color online) The plasma density profile in the plasma capillary. Upper plot shows 2D density profile in the capillary assuming axial symmetry. Also shown is the path of the pump propagation in vacuum in the experiments with tilted alignment of the laser beams. The pump pulse enters the channel from the left and the seed enters the plasma from the right. The lower plot shows the plasma density profile along the path of the pump beam in axial and tilted experiments [13,14].

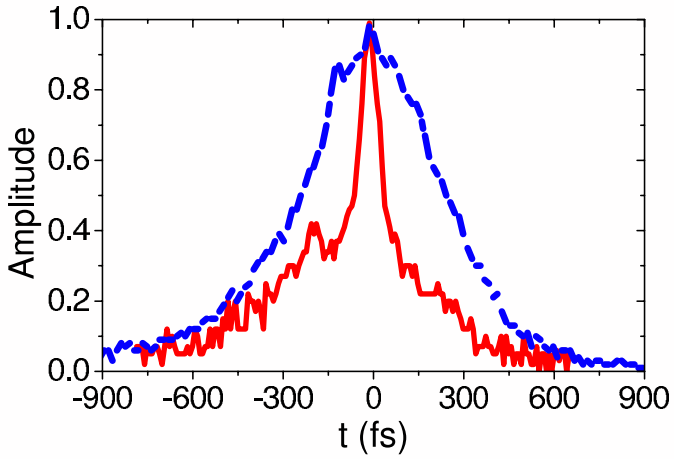

FIG. 3: (Color online) Amplified pulse (red solid line) and original seed pulse (blue dashed line) autocorrelation measurements in tilted experiments. The original 15 μJ 500 fs seed pulse is amplified by 77 mJ 20 ps pump and reaches the energy of 2.9 mJ. The autocorrelation measurements indicate that the output pulse has an intense spike and either the tail of the secondary spikes or a precursor. The duration of the main spike is about 90 fs and it contains about 50% of the total pulse energy [13,14].

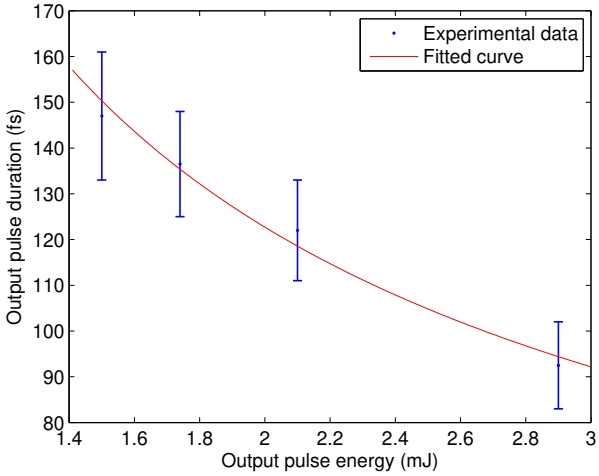

FIG. 4: (Color online) Scaling of the amplified seed duration with its energy. Solid line represents theoretical fit with $W^{\alpha}\Delta t$. A least mean square error fit gives $\alpha \approx 0.7$.

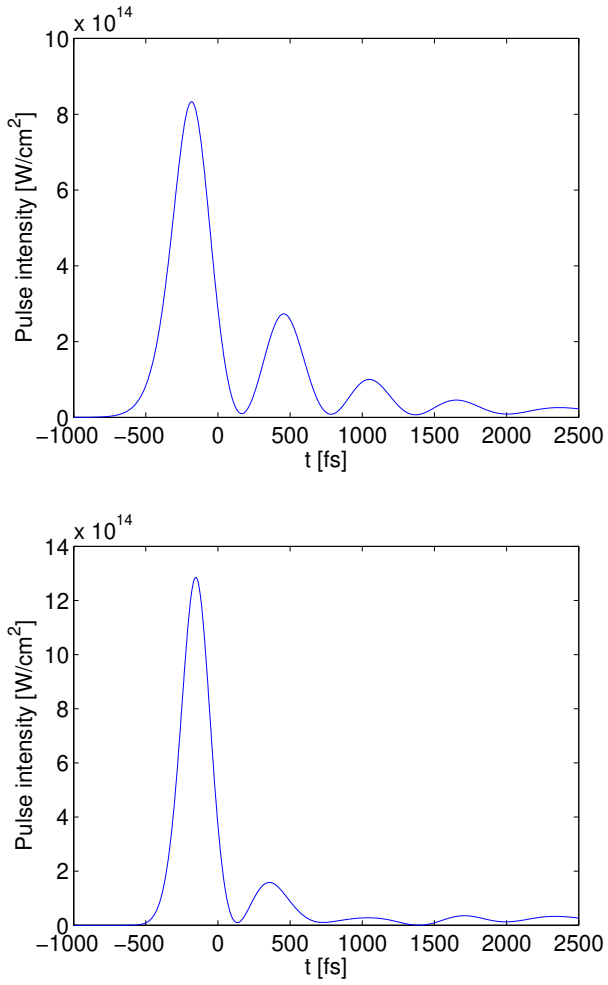

FIG. 5: (Color online) Simulated output amplified pulse intensity profile. The upper plot: the initial Gaussian seed of duration 500 fs and $\epsilon = 0.1$ is amplified in the uniform pump of intensity $I_{pump} = 2.5 \times 10^{14}$ W/cm^2 in $l = 2$mm plasma. Pump chirp $q = 1/4$. The overall efficiency of amplification $\int b^2 dt/(2a_0^2 l/c) = 13.6\%$. The lower plot: the seed pulse is the same as above but the tails of the Gaussian seed are truncated at 20% level. The output pulse is shorter and more intense than if the tails of the Gaussian seed are not suppressed.

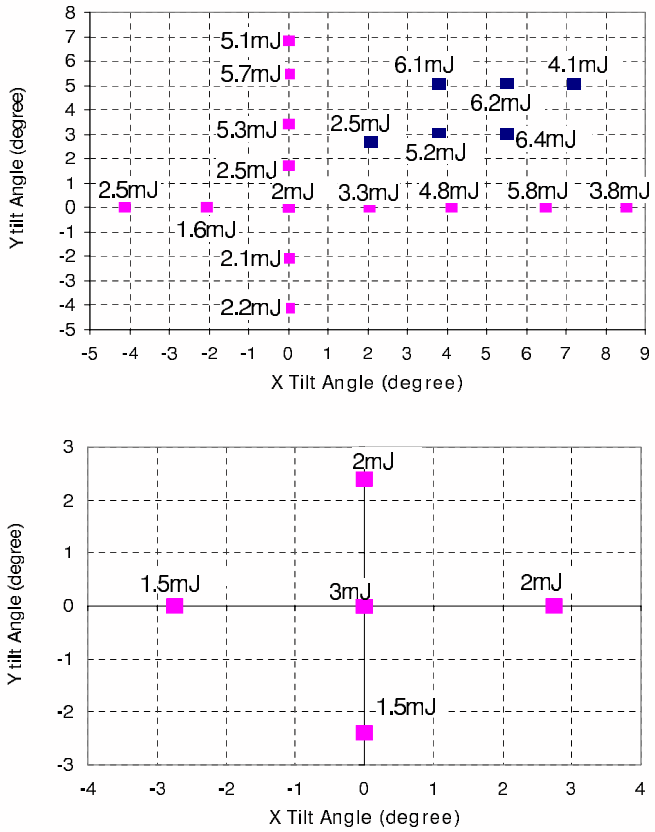

FIG. 6: (Color online) The upper plot shows the output energy of the amplified pulse in experiments with tilted geometry of the laser beams. Pump energy $W_{pump} \approx 100$ mJ, pump duration $\Delta t \approx 20$ ps, input seed energy $W_{seed} \approx 16$ mkJ, plasma channel length $l = 2$ mm. The tilt of the laser beams (both the pump and the seed pulses) is done with respect to the axis of the plasma channel. Lack of symmetry in x-y plane (tilt in horizontal and vertical direction across the channel) is not understood. We speculate that it is caused by misalignment of the laser beams due to refraction in the plasma channel. The lower plot shows the output energy in experiments with flipped sign of the pump chirp (negative chirp). Pump energy, pump duration, seed energy, and plasma channel length were the same as for the upper plot. The study of the negative pump chirp (lower plot) set up of the experiment is less complete than positive pump chirp set up. However, we observe the reduced efficiency in the tilted experiments compared to the axial experiments.

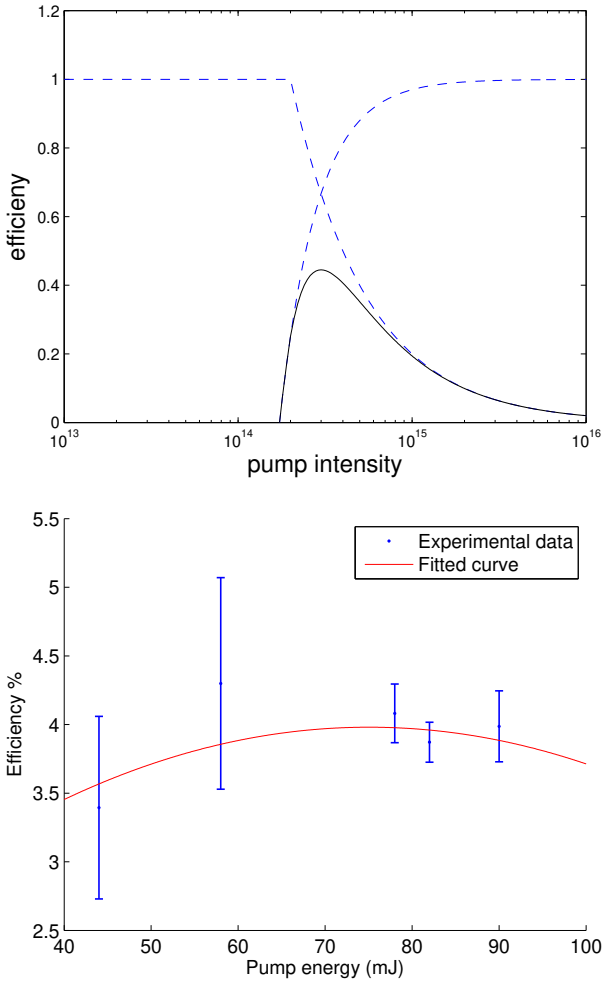

FIG. 7: (Color online) The upper plot shows theoretically estimated efficiency of BRA as described above. It has well defined maximum at a certain pump intensity. The lower plot shows experimentally measured dependence of the BRA efficiency versus the pump energy [14]. The intensity of the pump is proportional to the pump energy since the other parameters of the pump are fixed. The solid line is the least square parabolic fit of the experimental data points.

The Princeton Plasma Physics Laboratory is operated
by Princeton University under contract
with the U.S. Department of Energy.

Information Services
Princeton Plasma Physics Laboratory
P.O. Box 451
Princeton, NJ 08543

Phone: 609-243-2750
Fax: 609-243-2751
e-mail: pppl_info@pppl.gov
Internet Address: http://www.pppl.gov